URSI GASS 2020, Rome, Italy, 29 August - 5 September 2020

Cross-Correlation of Scattered GNSS Signals

Davide Comite* and Nazzareno Pierdicca
Department of Information Engineering, Electronics, Telecommunications,
"Sapienza" University of Rome, Italy

Abstract

Navigation signals reflected by the Earth surface, collected by a receiver in relative movement with respect to the source and the surface, can exhibit temporal fluctuations. Their features are related to the characteristics of the surface roughness and they can be observed even in the presence of almost flat surfaces with gentle undulations, i.e., those whose horizontal scale can be comparable with the impinging wavelength.

In this work, a full-wave solution of the scattering based on the Kirchhoff approximation is implemented to characterize the temporal variability of scattered signals of opportunity. A numerical solution is compared with a simple closed-form expression achieved considering omnidirectional sources. The analysis can provide useful information for the interpretation of GNSS data, especially those collected by means of satellite platforms, which presents an intrinsic variability that can significantly affect the retrieval of bio-geophysical parameters.

1 Introduction

Global Navigation Satellite Reflectometry (GNSS-R) signals reflected by natural surfaces, collected by an antenna looking downward, can be affected by losses of coherence [1], [2], [3]. A GNSS Reflectometer (GNSS-R) can be viewed as a *passive* radar system exploiting the illumination of one or more GPS transmitters to gather the reflections generated around the specular point on the surface [4], [5]. The scattered field at the receiver, indeed, in movement with respect to the illuminated surface, exhibits a decorrelation that is related to the system features (speed and height of the platform) and to the statistics features of the surface. The estimation of the bio-geophysical parameters of the illuminated surface by means of a GNSS-R sensor can be significantly affected by the temporal decorrelation of the scattering.

The scattered field can be assumed as the superimposition of an incoherent and a coherent contribution. The former has zero mean value and a random behavior, whilst the latter exhibits a well-defined phase pattern [6], [7], [8]. The incoherent contribution originates within the glistening zone, and it is described defining a bistatic normalized radar cross section (NRCS) [8]; the coherent one is generally assumed as originated by the specular reflection from an infinite mean surface (or other deterministic surface shape), and it can be described through the reflectivity [8], [9]. Their relative weight depends on the vertical and horizontal scale of the random roughness and by the amount of volume scattering (so that the phase information is lost).

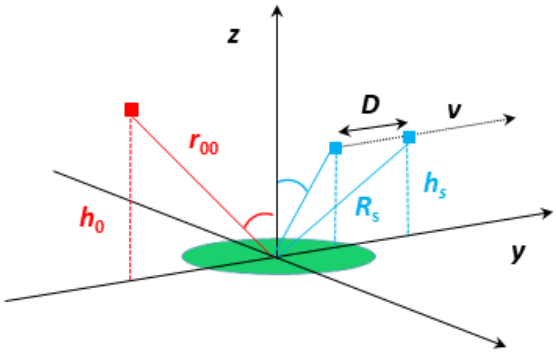

Figure 1. Geometry of a GNSS-R system. The receiver is moving within the forward quadrant. Both the antennas are aligned along the *y* axis; the incident (red) angle, the scattering angle (cyan), and the baseline *D* are also indicated.

Recently, with the increasing interest in the potential offered by GNSS-R receivers carried on satellite platforms [10], there has been an increasing demand for understanding the role of the surface topography, both in the presence of homogeneous and inhomogeneous media [7], [11]. An accurate characterization of the phenomenology of the scattering is also desirable to improve the retrieval performance [6], [12].

The dependence on system and physical parameters, as well as the intrinsic irregular repetition of the sampling point on the Earth surface (i.e., the specular point is hardly ever located in the same position even when acquiring data from the same orbit, and it moves as the satellite flies along the orbit), can strongly influence the behavior of the scattered signal both in the space and time domain. This determines the presence of temporal and spatial fluctuations, which can be observed even when the signal would be expected quite stable (i.e., as that generated by flat surfaces). To provide an accurate retrieval of the target quantities temporal oscillations must be mitigated and a proper strategy for the spatial and temporal aggregation of the signal should be designed. This includes the optimal choice of the coherent and incoherent integration typically performed by the data processor in order to reduce the additive random noise and to deal with more regular signals.

From an historical perspectives, similar analyses have also been performed to characterize acoustic signals scattered by pressure-release random surfaces, collected by an array of hydrophones [13], [14], as well as to characterize the coherence of Synthetic Aperture Radar (SAR) interferometric pairs as a function of the spatial baseline [2], [3]. In this work, a study of the temporal fluctuations of the signal collected by a moving GNSS-R receiver is proposed, comparing the analysis with a simple closed-form expression proposed in [15] in the frame of a scalar theory, considering omnidirectional acoustic sources.

2 Scattering Modeling

In real scenario, the electric field on the surface is produced by an antenna with a spherical wave front (locally plane in far field) and a power density angular distribution determined by the antenna pattern, which, for simplicity, can be assumed Gaussian or constant.

To characterize the temporal behavior of the field at the receiving point, we propose a one-dimensional (1-D) solution of the scattering considering the simple geometry reported in Fig. 1 (a 1-D random surface along the *y* axis described by a Gaussian random process is considered), where r_{00} and R_s represent the path lengths from the nominal specular point on the surface (i.e., the one associated to the mean plane surface) and the transmitting and receiving antennas, respectively. The Tx antenna is placed within the *yz* plane and illuminates the surface with a pointing angle θ_0 (measured with respect to the vertical axis, red color in Fig. 1); this defines a variable specular point with respect to the position of the receiver, which is in movement, along a linear direction and at a constant height H_s.

Under the Kirchhoff approximation (KA) [8], in the presence of a spherical incident wave, assuming small slopes, the field scattered by a 1-D rough surface is given by:

$$E_s = \frac{-jk_0}{4\pi}\int_{-\infty}^{+\infty} F(r)\left(\cos\theta_0+\cos\theta_s\right)\frac{e^{-jk_0(R_1+R_2)}}{R_1R_2}\mathrm{D}(y)dy \quad (1)$$

where D represents the shaping factor enforced by the antenna pattern. The radiated beam illuminates an area on the surface having approximate size equal to $R_0\beta_0/\cos\theta_0$. In (1), F(*r*) is the Fresnel reflection coefficient at the surface point indicated by *r=y* (computed according to the local incidence angle on the surface), k_0 is the wavenumber of the incident wave and *r=y* is the cartesian coordinate over the illuminated surface. R_1, R_2 are the distances of a generic point on the surface from the transmitting and receiving antenna.

The receiver is in movement at a constant height H_s (see Fig. 1), thus defining a variable observation zenith angle θ_s and an instantaneous baseline *D* (see Fig. 1). The transmitter is assumed steady (orbit at about 20.000 km). Depending on the speed *v* of the receiver, the scattered field is evaluated over *D*, up to a maximum distance dictated by *v*. Of course, the maximum distance is chosen to be much larger than the expected correlation time.

The decorrelation time of the collected signal, as the receiver moves along its trajectory, is numerically retrieved by solving the scattered electric field in (1) over a certain time interval, considering a Gaussian surface described by a correlation length *L* (i.e., the horizontal scale of the roughness) and an rms height σ (i.e., the vertical scale). The auto-covariance function of E_s is thus evaluated for increasing values of *D*, and the decorrelation time is estimated calculating the corresponding -3dB beamwidth, as described in the following:

$$\tau \;\Big|\; \left\langle E_s(t+\tau)E_s^*(t)\right\rangle \Big/ \left\langle \left|E_s(t)\right|^2\right\rangle = 0.5 \quad (2)$$

The value of τ represents the temporal interval for which the scattered field, under the considered illumination, keeps correlated or, equivalently, maintains its phase coherence. It describes a measure of the fluctuations to be expected for the non-averaged signals collected at the receiver. Note that smoother surfaces are expected to produce larger values of τ and that two limit conditions should be expected i.e., case of an uncorrelated surface ($L\to 0$) and of a perfect plane ($L\to\infty$).

As originally discussed in [1], [2], [3], and numerically validated in [12], a simple expression for the correlation time of an uncorrelated set of scatterers (that, in the limit, can be assimilated to an uncorrelated surface) is available, but no analytical solutions, to our best knowledge, exist for correlated surfaces and limited size of the illuminated area.

Considering finites values of *L* and an omnidirectional source (i.e., ideally non-truncated illuminations) placed at a radial distance r_{00} from the origin (see Fig. 1), performing a first-order approximation on the phase of the integral in (1), the autocorrelation of the scattered field was expressed in [15] as a function of the baseline *D*, as given in the following:

$$\left\langle E_s(t+\tau)E_s^*(t)\right\rangle = \mathrm{A}_0 \mathrm{e}^{-4k_0^2\sigma^2\sin^2(\theta_{sp})\left[1-\Psi(2\mu_y)\right]} \quad (3)$$

where θ_{sp} is the specular point defined with respect to the baseline midpoint *D* [15]. $\Psi(\mu_y)$ in (3) represents the autocorrelation function of the surface (that is typically assumed Gaussian or exponential), while μ_y reads as

$$\mu_y = \frac{D}{2}\left(\frac{r_{00}}{r_{00}+r_{10}}\right) \quad (4)$$

where r_{10}, following the notation in [15], is the radial distance of the baseline midpoint measured with respect to the origin of the reference system. This formulation, developed for an acoustic type of problem, is compared here with a numerical solution of eq. (1) conceived for a microwave GNSS-R type of measurement.

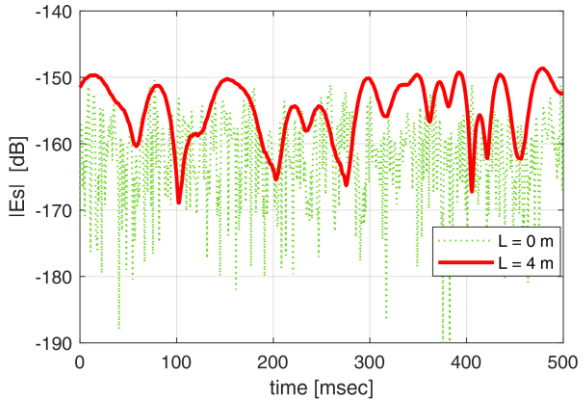

Figure 2. Amplitude vs. the time of the monocromatic scattered field for two values of L and one representative value of surface rms heights, σ = 6 cm.

3 Numerical Results

A set of surface profile within a variable range of spatial correlation (from small values to larger values, thus including random surfaces characterized by gentle undulations at larger scale) have been simulated numerically solving the integral in (1). A few values for the surface rms height have also been considered, in the order of few centimeters to 26 centimeters. This has been done to represent smooth terrains that are not exactly flat but can exhibit a height variation with relatively long horizontal scales (i.e., long correlation lengths). These undulations cannot be appreciated by visual inspection or even described by a Digital Elevation Model (DEM), so that the targeted surface could be labelled as "flat". Nevertheless, they can generate interferences in a coherent microwave system, whose presence can be quantified by calculating the correlation time as given by (2).

A surface having permittivity equal to $\varepsilon_r = 6 - j0.6$ is considered. The total beamwidth of the transmitting and receiving antennas are set to 45° and 30°, respectively. This determines a finite illumination over the surface, which, for simplicity, is set constant here. The receiver is assumed aboard of a small plane, flying at a height equal to 100 m. The spherical-wave illumination is set at R_0 = 20 000 km with θ_0 = 15°. The results presented are achieved considering an L-band system (f = 1.57 GHz). The numerical integral is carried out by sampling the surface with a resolution of one seventh of the wavelength.

All the considered surfaces have been synthesized assuming a Gaussian correlation function and implementing a Monte Carlo approach based on 25 determinations of the relevant random process to come with a smoother averaged trend of the correlation time as a function of the surface correlation length. Only 1-D surfaces and low platforms have been considered. Simulations of satellite altitudes require to sample of a larger area with a resolution in the order of a fraction of the wavelength, making the computational time very long.

Figure 2 reports the amplitude of the scattered field collected by the receiver moving along the track (i.e., over the baseline of the system), for two different values of L and σ. Stronger temporal fluctuations of the scattered field are observed for surfaces that are spatially less correlated (i.e., for smaller L). Conversely, the scattered field amplitude temporal behavior is much smoother for longer correlation length (L = 4 m). The vertical standard deviation is σ = 6 cm, thus the slopes of the surface are very small, difficult to distinguish from a plane surface.

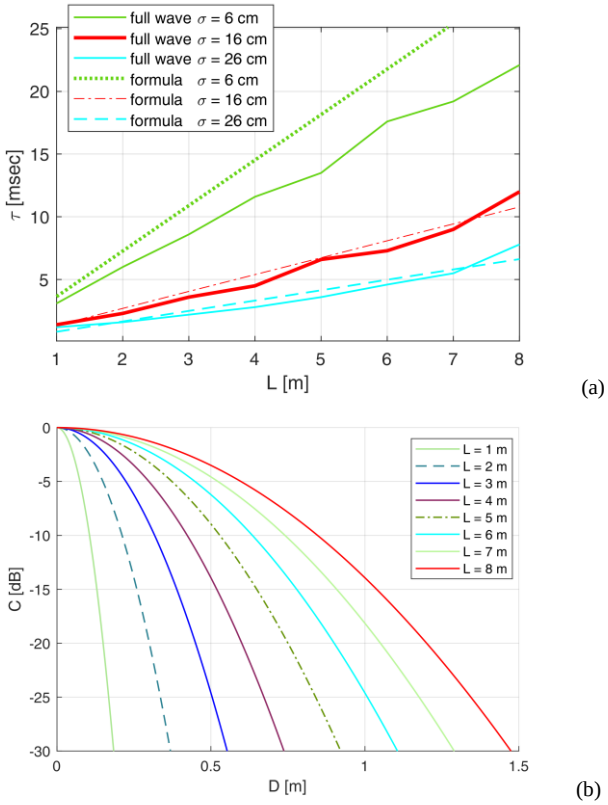

Figure 3. (a) Electric field correlation time vs. the surface correlation length for different values of the surface rms heights: comparison between numerical experiments and the expression in (3).
(b) Autocorrelation function vs. the baseline D of the scattered field for different values of L and σ = 16 cm.

Figure 3(a) reports the correlation time achieved numerically as dictated by (2) versus the surface correlation length for different values of the surface roughness. The numerical data show a monotonic increment of the correlation time with L, which gradually determines a gentler surface. Note that these values of τ, especially for small L, are of the order of the coherent integration time assumed in the processing of many airborne sensors and of current spaceborne GNSS-R receivers (such as CYGNSS and TechDemoSAT-1) [10]. Note also that by extrapolating the simulated results to L→0 we get a correlation time of about 2 msec for a rough surfave (large σ). This value is very much close to the one that can be derived from available model for an uncorrelated distribution of scatterers [1].

Figure 3(a) also reports a comparison between the numerical τ with those achieved by implementing equation (3). The autocorrelation of the field versus the baseline D

obtained by equation (3) is reported in Fig. 3(b), showing a wider pattern for increasing values of *L*. The agreement between numerical simulations and the closed-form expression in Fig. 3(a) is rather good, testifying that such simple expression is able to satisfactorily model the background physics of the problem, at least for this specific configuration and illumination.

Further works are in progress to analyze the effect of the receiver altitude as well as to retrieve a closed-form expression capable of incorporating the effect of a finite illumination, an aspect that can assume more importance at satellite altitudes and in case of systems having a finer spatial discrimination (i.e., spatial resolution).

4 Conclusions

Temporal fluctuations of GNSS signals, associated to the quasi-specular reflections over land and determined by the presence of gentle undulations (i.e., relatively small vertical displacement over a long horizontal scale) of the surface, have been investigated in this contribution. The correlation time of the GNSS-R signal as a function of the statistical properties of the surface (height standard deviation and correlation length) and the geometry of the acquisition (height, velocity) has been numerically evaluated, comparing the results with a simple closed-form expression achieved considering the illumination of omnidirectional sources. It has been discussed that the temporal decorrelation of the field can be strongly dependent on the features of the illuminated surface, but also on the receiver speed.

The topic may be interesting for an accurate interpretation and processing of the GNSS-R data, either airborne or spaceborne. Further analysis should be performed to assess the role of the geometry and of system parameters, also accounting for satellite-borne receivers.

5 Acknowledgements

This work was partially supported by ESA in the framework of the projects "Potential of Spaceborne GNSS-R for Land Applications" under Contract 4000120299/17/NL/AF/hh.

6 References

1. C. Zuffada, T. Elfouhaily, and S. Lowe, "Sensitivity analysis of wind vector measurements from ocean reflected GPS signals," *Remote Sens. Environ.*, **88**, 3, pp- 341-350, May 2003.

2. G. Franceschetti, et al., "The effect of surface scattering on IFSAR baseline decorrelation," *J. Electromagnetic Waves Applications*, **11**, 3, pp. 353-370, 1997.

3. H. A. Zebker and J. Villasenor, "Decorrelation in interferometric radar echoes," *IEEE Trans. Geosci. Remote Sens.*, **30**, 5, pp. 950-959, Sep. 1992.

4. F. Martín, A. Camps, H. Park, S. D'Addio, and M. Martín-Neira, D., "Pascual Cross-correlation waveform analysis for conventional and interferometric GNSS-R approaches," *IEEE J. Sel. Topics Appl. Earth Obs. Remote Sens.*, **7**, 5, pp. 1560-72, Feb. 2014.

5. V. U. Zavorotny, S. Gleason, E. Cardellach, and A. Camps "Tutorial on remote sensing using GNSS bistatic radar of opportunity," *IEEE Geosci. Remote Sens. Mag.*, **2**, 4, pp. 8-45, Dec. 2014.

6. H. You, J. L. Garrison, G. Heckler, and V. U. Zavorotny, "Stochastic voltage model and experimental measurement of ocean-scattered GPS signal statistics," *IEEE Trans. Geosci. and Remote Sens.*, **42**, 10, pp. 2160-2169, Oct. 2004.

7. A. M. Balakhder, M. M. Al-Khaldi, and J. T. Johnson, "On the coherency of ocean and land surface specular scattering for GNSS-R and signals of opportunity systems," *IEEE Trans. Geosci. Remote Sens.*, **57**, 12, pp. 10426-1036, Sep. 2019.

8. F. T. Ulaby, R. K. Moore, and A. K. Fung, *Microwave Remote Sensing Active and Passive-Volume II: Radar Remote Sensing and Surface Scattering and Enission Theory*. Artech House Publishers, 1986.

9. D. Comite, F. Ticconi, L. Dente, L. Guerriero, and N. Pierdicca, "Bistatic coherent scattering from rough soils with application to GNSS reflectometry," *IEEE Trans. Geosci. Remote Sens.*, **58**, 1, pp. 612-625, Jan. 2020.

10. M. Unwin, P. Jales, J. Tye, C. Gommenginger, G. Foti, and J. Rosello, "Spaceborne GNSS-reflectometry on TechDemoSat-1: Early mission operations and exploitation," *IEEE J. Sel. Topics Appl. Earth Obs. Remote Sens.*, **9**, 10, pp. 4525-4539, Sep. 2016.

11. L. Dente, L. Guerriero, D. Comite, and N. Pierdicca, "Space-borne GNSS-R signal over a complex topography: Modelling and validation," *IEEE J. Sel. Topics Appl. Earth Obs. Remote Sens.*, Jan. 2020, in press.

12. D. Comite, L. Dente, L. Guerriero, and N. Pierdicca, "Modeling the coherence of scattered signals of opportunity," *Proc. IEEE Int. Conf. Geosci. Remote Sens*, Jul. 2019, pp. 4819-4822.

13. S. T. McDaniel, "Spatial covariance and adaptive beam forming of high-frequency acoustic signals forward scattered from the sea surface," *IEEE J. Oceanic Eng.*, **16**, 4, pp. 415-419, 1991.

14. J. M. Restrepo and S. T. McDaniel, "Two models for the spatially covariant field scattered by randomly rough pressure-release surfaces with Gaussian spectra," *J. Acoustical Soc. Am.*, **87**, 5, pp. 2033-2043, 1990.

15. J. P. Welton, "Cross correlation of omnidirectional, broadband signals scattered by a random pressure-release surface." *IEEE J. Oceanic Eng.*, **40**, 2, 485-494, 2014.